Implantable Multichannel Electrode Array Based on SOI Technology

Karen C. Cheung, Kaj Djupsund, Yang Dan, and Luke P. Lee

***Abstract*—This work presents a new method of fabricating implantable multielectrode arrays on lightly doped single-crystal silicon. Such arrays are essential tools for electrical stimulation and recording of nerve signals. Our new microfabrication process, based on silicon-on-insulator (SOI) technology, inherently has excellent control over the final probe thickness without wet etching. The needle shanks are 6 mm long and 80 μm wide. Here the thickness of the probe, 25 μm, is defined by the device layer thickness on the SOI wafer. Our new sprinkler fluidic channel, which has holes spaced 50 μm apart along its 6 mm length, permits the perfusion of a large area of tissue with any desired neurotransmitter or other drug. The probes fabricated here are tested in the cat primary visual cortex; data recorded from adjacent neurons was used to characterize their orientation tuning. The sprinkler channel was characterized, and flowrate through the channel is a linear function of the applied pressure. [872]**

***Index Terms*—Implantable multielectrode array, neural probe, silicon-on-insulator (SOI).**

I. Introduction

IMPLANTABLE microelectrode arrays will contribute enormously to the understanding of how sensory stimuli are processed in the brain. Microfabrication allows the batch production of these tools with reproducible characteristics. In addition, microfabrication technologies permit the design and realization of more complicated probe geometries than traditional glass electrode setups. These new neural probes record electrical responses at the cellular level, and analysis of a network of cells will help to elucidate how the neural code builds a representation of the external environment.

At present, several neural probes allow simultaneous electrical stimulation and recording, as well as chemical stimulation. The integration of a fluidic channel into the probe permits highly localized injection of neurotransmitters or other drugs. This added functionality allows a biomimetic approach and potentially has many long term applications. The fluidic outlets can be located right at the electrical recording site or at intervals a precise distance away from the recording site.

In this paper we present a new method of fabricating implantable multielectrode arrays with integrated fluidic channels using silicon-on-insulator (SOI) wafers. Previous probe designs have concentrated the injection sites at a single depth. With the new sprinkler channel design, which has holes along the length of the channel, a large area of tissue can be perfused with the desired drug. Since many cellular receptors in the brain are organized in layers, with inputs and outputs from each cell targeting different cortical layers, a one-point injection site can be relatively insensitive or create a variable effect. A sprinkler channel in this case will equalize the effects of an injected agent along the sensor array. The probes fabricated here are tested in the cat primary visual cortex.

Manuscript received May 16, 2002; revised November 7, 2002. This work was supported by a grant from the Whitaker foundation. Subject Editor K. D. Wise.

K. C. Cheung and L. P. Lee are with the Berkeley Sensor and Actuator Center, Department of Bioengineering, University of California at Berkeley, Berkeley, CA 94720-1774 USA (e-mail: lplee@socrates.berkeley.edu).

K. Djupsund and Y. Dan are with the Department of Molecular and Cell Biology, Neuroscience, University of California at Berkeley, Berkeley, CA 94720-1774 USA.

Digital Object Identifier 10.1109/JMEMS.2003.809962

II. Probe Fabrication Using SOI Technology

SOI wafers separate a thin silicon device layer, which can range in thickness from 1 μm to 100 μm, from the silicon substrate using a buried insulating layer. The insulating layer, which can be 1 to 2 μm in thickness, is usually silicon dioxide and is called the buried oxide. This wafer structure presents several advantages for the fabrication of integrated circuits, including the minimization of leakage current and junction capacitance, and robustness against transient radiation effects [1]. In the MEMS realm, SOI is a convenient substrate for the production of single-crystal structures, such as piezoresistive pressure sensors and capacitive accelerometers [2]. Although the first generations of SOI wafers were quite expensive, the cost of such substrates is going down with the advent of new wafer production methods. Many companies produce SOI wafers with standard device layer thicknesses, such as 25, 50, 75, or 100 μm, which can be readily purchased. Custom layer thicknesses are of course available with longer lead times.

In previous neural probe fabrication schemes, the probe shanks were defined using highly boron-doped silicon, which is almost unattacked in anisotropic etchants such as ethylamine-diamine pyrocatechol (EDP) [3]–[9]. Since the final release of those structures is in a wet etch bath, there is a risk of destroying any on-chip CMOS devices in the case of over-etch, and special precautions must be taken to protect the circuitry [10]. Other processes use only plasma etching to define the probe shape [11].

One of the key issues in microelectrode array design is probe miniaturization, to minimize disruption of the surrounding neural tissue [12]. Our new microfabrication process, based on SOI technology, inherently has excellent control over the final probe thickness without wet etching, because the thickness of the probe is defined by the device layer thickness on the SOI wafer. The buried oxide acts as an etch stop during a backside deep reactive ion etch (DRIE) of the wafer. This silicon etch is extremely selective to silicon dioxide (120:1 against silicon dioxide) and stops at the buried oxide. During the backside

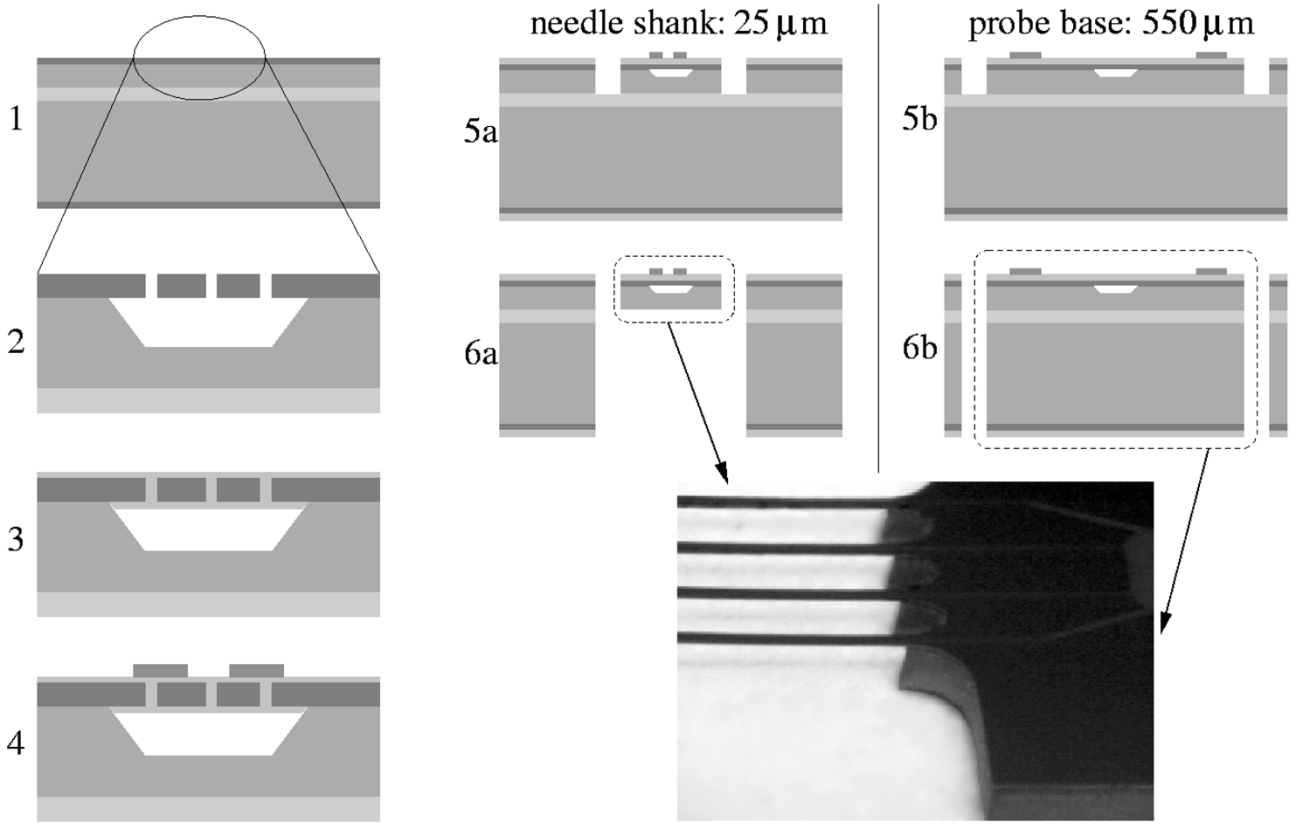

Fig. 1. Probe fabrication steps: 1. Start with a 25-μm SOI wafer, deposit nitride. (Steps 2–4 focus on the device layer of the SOI wafer) 2. Pattern the nitride so that wet etchant can create the buried channel. 3. Deposit oxide to close up the access holes. 4. Pattern the electrodes by lift-off and passivate. 5. A front-side DRIE defines the probe outline. 6. A back-side DRIE completes the probe structure. In 6a, the wafer is thinned to the BOX under the thin needles. In 6b, the entire wafer thickness remains under the bond bad and fluidic inlet area.

etch, the silicon substrate is removed from underneath the probes; thus the final probe thickness is determined by the thickness of the silicon device layer.

III. Materials and Methods

A. Fabrication of Multielectrode Arrays With Integrated Fluidic Channels

The neural probes were fabricated on a 25-μm SOI wafer (see Fig. 1) with 1 μm buried oxide. The first steps in the process deal with the formation of fluidic channels, which are buried beneath the surface of the wafer. A 0.5-μm-layer of silicon nitride was deposited on the wafer using low-pressure chemical vapor deposition (LPCVD). The channels are defined by arrays of 1 μm holes that are patterned on the nitride using standard photolithographic techniques. The channel inlets and outlets are arrays of 3 μm holes patterned in the same manner (see Fig. 2). The holes are etched into the nitride in a reactive ion etch (RIE) using CF_4 and CHF_3. The wafer was immersed in a wet silicon etchant ($126\ HNO_3 : 60\ H_2O : 5\ NH_4F$, room temperature) for 30 min. This resulted in an isotropic etch of the silicon underneath the holes. A subsequent etch in KOH ($1\ KOH : 2\ H_2O$ by weight, 80 °C), an anisotropic etchant, completed the trapezoidal channels. The wet etching is followed by the deposition of 2 μm of oxide by LPCVD. This deposition closed the 1 μm holes that defined the channels, but left the larger inlet and outlet holes open.

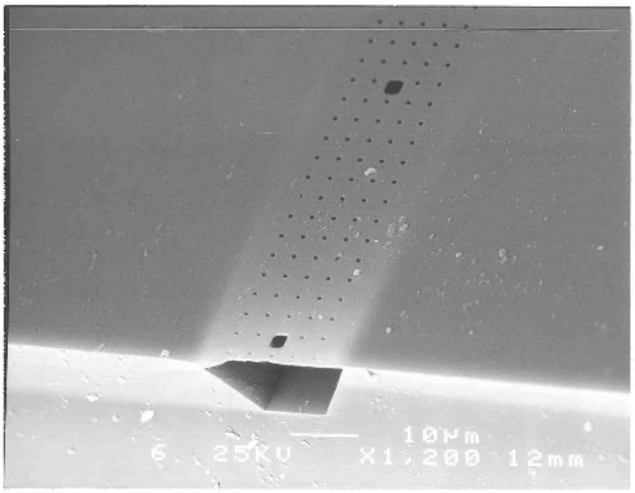

Fig. 2. Fluidic channel after wet etching and before LPCVD oxide redeposition. The smaller 1 μm holes that define the channel are eventually closed up after redeposition of oxide. The 3 μm holes shown here are arranged in a "sprinkler" design, so that a neurotransmitter can be perfused into a large area of tissue.

The next process steps deal with the patterning of electrodes and their insulation. The electrodes were made using the lift-off method: the photoresist was patterned, and a 1000-Å layer of platinum was sputtered on top of a thin chrome adhesion layer. The metal features are defined in an ultrasonic bath in acetone. A 3500-Å layer of plasma-enhanced chemical vapor deposition

(PECVD) silicon nitride was deposited on top of the entire wafer for electrical insulation. Contact areas to the platinum electrodes were etched through the nitride in an SF_6 RIE.

The final steps in the process define the probe shape. The outline of the probes was etched on the front side of the wafer in a deep-reactive ion etch (DRIE) using SF_6 (Surface Technology Systems, UK). The etch went through the entire thickness of the silicon device layer on the SOI, stopping on the buried oxide. The back side of the SOI wafer was then patterned with the probe outline. Using a back-side DRIE that stopped on the buried oxide, the multielectrode arrays were defined so that only the 25-μm device silicon layer remains at the needle-shaped probes. In contrast, the contact pad area was unetched and remained at the original wafer thickness. The buried oxide was removed from the backs of the probes using a plasma etch.

The completed multielectrode arrays were glued to a custom-made circuit board. The contact pads on the electrodes were wirebonded using aluminum wire, and the circuit board was soldered to pins so that the entire package could be connected to a standard connector for ease in data acquisition. Polyimide tubing was glued to the fluidic inlet and connected to a syringe pump.

In this fabrication method, the thickness of the device silicon layer on the SOI wafer determines the thickness of the finished probes. By making use of the SOI wafer structure, this process has inherent control over the final probe thickness. In addition, by selectively etching the backside of the wafer, the product can contain components which are at the original wafer thickness. This is especially convenient since it gives ease in handling and wirebonding. Here the probes are 25 μm thick while the electrode pad area remains at the thickness of the entire SOI wafer (550 μm). Since these SOI wafers were made by bonding a thin double-polished silicon wafer to an oxidized handle wafer, the backs of the probes are very smooth.

B. Testing in the Visual System

The functionality of the new multielectrode array was tested on the visual cortex of adult cats ranging from 2.5 to 3.5 kg. Cortical cells from layers II–IV were recorded. The cat was first anesthetized with isofluorane and then with sodium pentobarbitol; lidocaine, a local anesthetic, was injected before all incisions. A tracheostomy was performed to allow artificial respiration. The cat was then put on a Horsley-Clarke stereotaxic frame. A craniotomy (approximately 0.25 cm^2) was performed over the primary visual cortex, and the underlying dura was removed. Pupils were dilated with a topical application of atropine sulfate. The eyes were fitted with contact lenses and focused on a tangent screen. The cats were paralyzed and artifically respirated. The core body temperature was monitored and maintained at 38 °C, while the electrocardiogram and electroencephalogram were also monitored continuously during the experiment. The eye positions were mechanically stabilized by gluing the sclerae to metal posts attached to the stereotaxic apparatus. The multielectrode array was attached to a motorized micromanipulator (Soma, Inc.) for the insertion in the brain. Visual stimuli were created on a personal computer. The stimuli consisted of parallel black and white bars that moved across the screen. In order to find the orientation axis of the cells' receptive fields, these gratings were rotated around 360° in 15 or 30° steps. The cells' responses to the moving gratings were measured, and the frequency of action potentials was recorded as a function of the orientation of the bars. Recorded signals were amplified, filtered, and passed to a personal computer. The on- and off-line analysis of the recordings were performed with commercial and custom-made software (Visual C, Matlab 6.1, LabTalk).

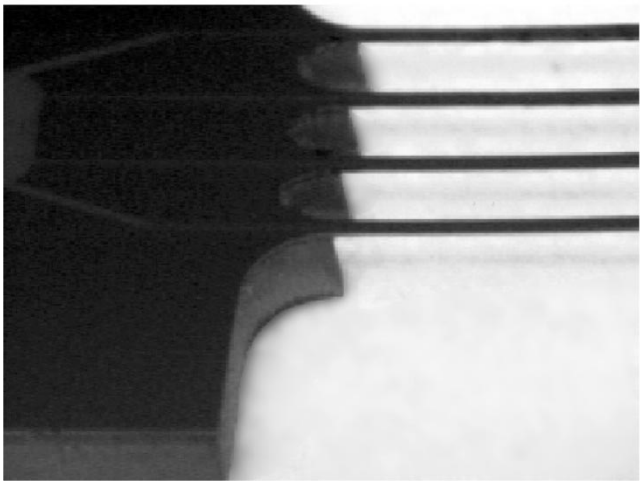

Fig. 3. Needle shanks are 6 mm long and 80 μm wide. The contrast between the 25 μm thick needles and the 550 μm thick handle area is evident. Each probe has one fluidic channel that runs down its length. The four channels connect at the base of the probe at the inlet area.

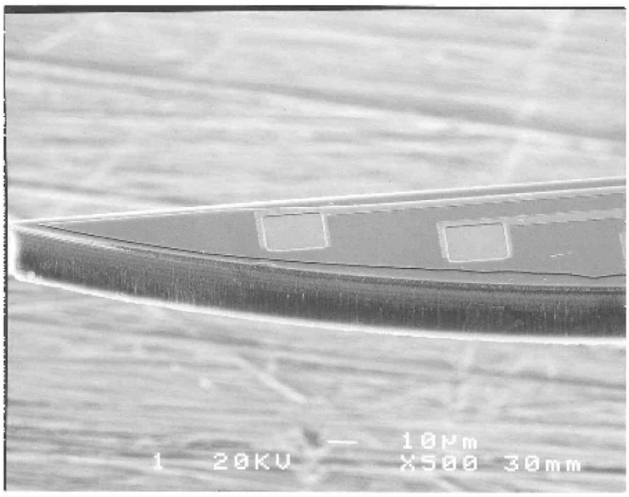

Fig. 4. Electrodes at the tip of each probe are separated by 45 μm spacing. Each electrode is 20 μm $\times$ 20 μm square.

IV. Results and Discussion

A. Probe Structures

The 25-μm thickness was chosen since this is a readily available wafer type. The increased thickness should provide increased stiffness when compared to previous boron-doped probes, which are approximately 12 μm thick.

The needle shanks are 6 mm long and 80 μm wide. Each multielectrode array has four needles (Fig. 3), and each needle has four electrodes spaced 45 μm apart along its length. Although the needle shanks are spaced 340 μm apart here, the spacing can

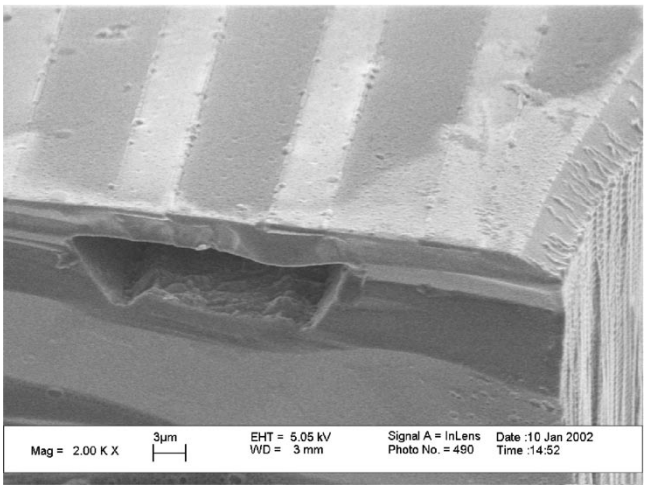

Fig. 5. Close-up view of a trapezoidal channel. The four lines above the channel are platinum insulated by silicon nitride.

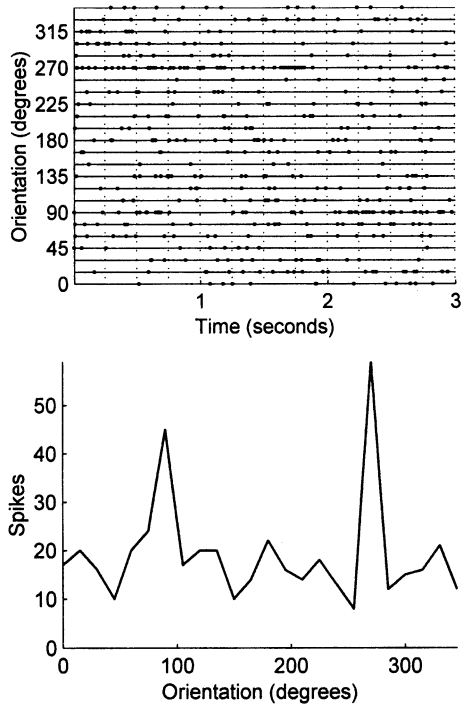

Fig. 6. Recording of typical cell discharges from one channel shows the direction tuning of a cell.

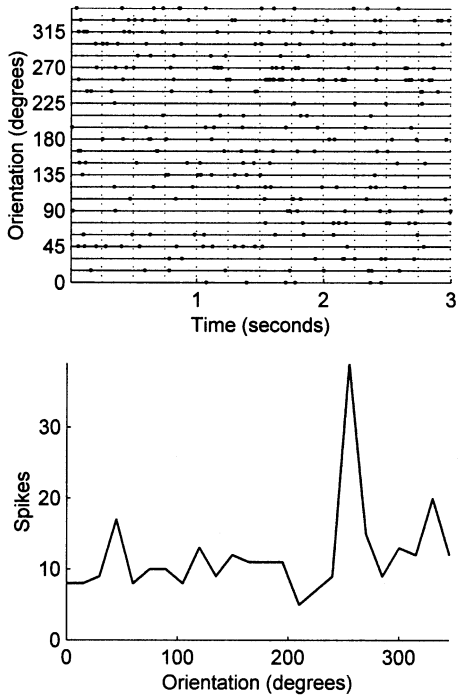

Fig. 7. Recording of typical cell discharges from another channel shows that this cell has a different direction tuning.

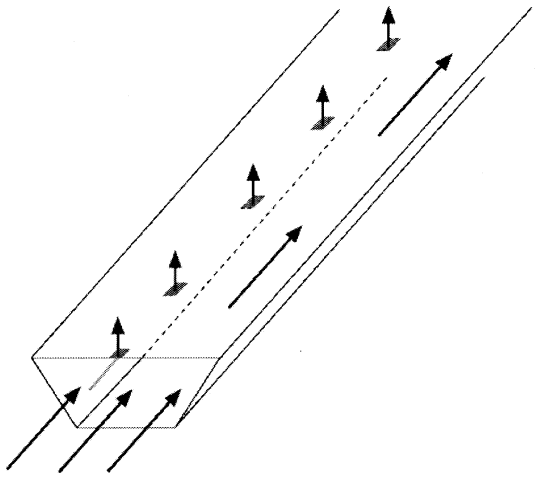

Fig. 8. The sprinkler channel.

be less than 50 μm. The electrodes are 20 μm $\times$ 20 μm squares (see Fig. 4). The channel has a trapezoidal cross section, with a hydraulic radius of 8.5 μm (see Fig. 5).

B. Testing in the Visual System

The cells in the visual cortex are roughly divided into simple and complex cells. Whereas simple cells tend to have clear discrete excitatory and inhibitory zones, complex cells lack these within their receptive field. Both types commonly show a preference to orientation or even direction of stimulating gratings, and the response of a cell (i.e., the number of action potentials fired) is at maximum for stimuli of these directions. When positioned adjacent to one or several of these cells, the multielectrode array can be used to characterize their orientation tuning (see Figs. 6 and 7).

The probes were designed with a triangular, knife-like shape at the tip to facilitate travel through the whole depth of the cortex. The flexibility of the thin silicon probes is a compromise between mechanical durability and targeting precision. While the probe stiffness will increase with increasing thickness, a thicker probe will also destroy or displace more tissue during insertion. Although the electrodes do bend during insertion into the cortex, there are several other uncertainties in targeting accuracy, such as error factors in the stereotactic apparatus and individual differences in brain structure. However, the probe bending should not affect the targeting of nuclei over 1 mm in diameter.

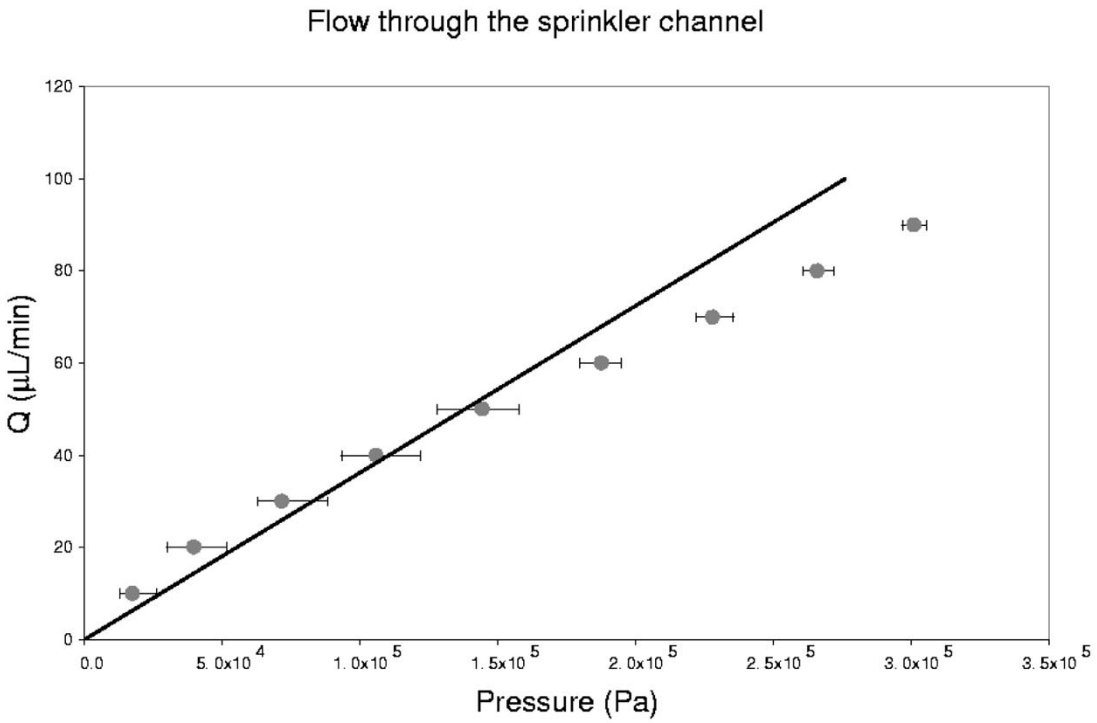

Fig. 9. Flow through the sprinkler channel. The zeroth order perturbation solution is plotted as the solid line. Data from several channels fits with the predicted profile.

C. The Sprinkler Fluidic Channel

The sprinkler fluidic channel has holes along its length which permit perfusion of the injected neurotransmitter into a large area of tissue (see Fig. 8). Channel dimensions are reproducible as long as the silicon etching agents ($126\ HNO_3 : 60\ H_2O : 5\ NH_4F$, room temperature) and KOH solution ($1\ KOH : 2\ H_2O$ by weight, 80 °C) are freshly mixed prior to each usage and agitated during the etching times. The flow through this fluidic channel is expected to be laminar.

Since the radial flow out of the channel is expected to be small due to the length L of the channel relative to the channel radius R, the internal flow should be perturbed only slightly from the Poiseuille solution. Using $\varepsilon = R/L$ as the perturbation parameter in a regular perturbation analysis, the zeroth order solution gives the flowrate Q:

$$Q = \frac{wK}{\lambda \sinh \lambda}(\cosh \lambda - 1)(\Delta P) \tag{1}$$

where Q is the leakage flow out of the holes along the length of the channel. Here

$$\lambda = 4\sqrt{\frac{K\mu}{\varepsilon^2 R}} \tag{2}$$

where K is the permeability through the porous channel wall, μ is the viscosity of the fluid, and ε is the aspect ratio of the channel.

The pressure drop through the channels was measured using a flow-through pressure transducer (Honeywell). Flow was controlled using a syringe pump (Cole Parmer) set at flowrates from 10–120 μL/min. Data from several channels fits closely with the profile predicted by the zeroth order perturbation solution (see Fig. 9).

V. Conclusion

This new microfabrication process, based on SOI technology, inherently has excellent control over the final probe thickness without wet etching, because the thickness of the probe is defined by the device layer thickness on the SOI wafer. This fabrication process requires only reactive ion etching to define the probe outline and will be compatible with the eventual addition of on-board electronics for signal amplification and multiplexing. The probes were able to record signals from adjacent neurons, and the data is used to characterize their orientation tuning. The sprinkler channel was characterized and flowrate through the channel is a linear function of the applied pressure. It can be used to perfuse large areas of tissue with the desired neurotransmitter. Since injected fluid will probably spread horizontally along and within membrane spaces in the brain, this probe design might be well suited for use in cases such as the mouse hippocampus, which has a large number of tough structures, horizontal membranes and cavities, and intricate folds, and which is reachable with a 5-mm-long needle shank.

Future work will include monitoring the impedance of the electrode sites over time, to examine the electrode and nitride insulation layer stability. One of the difficulties still to be surmounted in many microdevices is the fluidic connection. In addition, any particulates in the fluid will obstruct the channel and render it unuseable; the fluid must be filtered to remove dust and any species which might have crystallized out of solution. In the future, a complete probe system will have integrated pumps and valves for precise fluidic control.

Biocompatibility is an important issue in the fabrication of microelectrodes since such a recording/stimulation system should not evoke significant tissue reaction in vivo. The million-fold difference in stiffness between a silicon-based probe and the surrounding tissue (190 GPa versus 0.1 MPa) can cause significant differential movement in response to external stress, which contributes to fibrous encapsulation and chronic astrogliosis. At present, silicon substrates provide many advantages for the production of neural probes because the microfabrication processes are well developed. However, the next generation of implantable neural probes will be those which provide a better mechanical impedance match between probe and tissue.

ACKNOWLEDGMENT

All microfabrication was performed at the University of California at Berkeley Microfabrication Laboratory. All animal experiments were performed as approved by the Animal Care and Use Committee, University of California at Berkeley.

REFERENCES

[1] S. Cristoloveanu, "Silicon on insulator technologies and devices: from present to future," *Solid-State Electron.*, vol. 45, no. 8, pp. 1403–1411, Aug. 2001.
[2] S. Renard, "Industrial MEMS on SOI," *J. Micromechan. Microeng.*, vol. 10, no. 2, pp. 245–249, June 2000.
[3] J. Chen, K. D. Wise, J. F. Hetke, and S. C. Bledsoe, "A multichannel neural probe for selective chemical delivery at the cellular level," *IEEE Trans. Biomed. Eng.*, vol. 44, no. 8, pp. 760–769, Aug. 1997.
[4] Q. Bai, K. D. Wise, and D. J. Anderson, "A high-yield microassembly structure for 3-D microelectrode arrays," *IEEE Trans. Biomed. Eng.*, vol. 47, no. 3, pp. 281–289, Mar. 2000.
[5] C. Kim and K. D. Wise, "A 64-site multishank CMOS low-profile neural stimulating probe," *IEEE J. Solid-State Circuits*, vol. 31, no. 9, pp. 1230–1238, Sept. 1996.
[6] K. D. Wise and K. Najafi, "Microfabrication techniques for integrated sensors and microsystems," *Science*, vol. 254, no. 5036, pp. 1335–1342, Nov., 29 1991.
[7] Y. B. Gianchandani and K. Najafi, "A bulk silicon dissolved wafer process for microelectromechanical devices," *J. Microelectromech. Syst.*, vol. 1, no. 2, pp. 77–85, June 1992.
[8] K. Najafi, J. Ji, and K. D. Wise, "Scaling limitations of silicon multichannel recording probes," *IEEE Trans. Biomed. Eng.*, vol. 37, no. 1, pp. 1–11, Jan. 1990.
[9] K. Najafi and K. Suzuki, "Measurement of fracture stress, Young's modulus, and intrinsic stress of heavily boron-doped silicon microstructures," *Thin Solid Films*, vol. 181, pp. 251–258, Dec. 1989.
[10] Q. Bai and K. D. Wise, "Single-unit neural recording with active microelectrode arrays," *IEEE Trans. Biomed. Eng.*, vol. 48, no. 8, pp. 911–920, Aug. 2001.
[11] D. T. Kewley, J. M. Bower, M. D. Hills, D. A. Borkholder, I. E. Opris, N. I. Maluf, C. W. Storment, and G. T. A. Kovacs, "Plasma-etched neural probes," *Sens. Actuators, Phys. A*, vol. 58, no. 1, pp. 27–35, Jan. 1997.
[12] D. J. Edell, V. V. Toi, V. M. McNeil, and L. D. Clark, "Factors influencing the biocompatibility of insertable silicon microshafts in cerebral cortex," *IEEE Trans. Biomed. Eng.*, vol. 39, no. 6, pp. 635–643, 1992.

Karen C. Cheung received the Ph.D. degree in bioengineering from the University of California at Berkeley in 2002, as a Whitaker Graduate Fellow. The subjects of the dissertation project included implantable neuroMEMS and microscale neural interfaces.

She is currently a Postdoctoral Researcher at the Swiss Federal Institute of Technology, Lausanne.

Kaj Djupsund received the M.D., M.S.E.E., and Ph.D. degrees from the University of Oulu, Finland.

He participated in this work at the University of California, Berkeley, in 2000–2001 and is currently a researcher at the University of Kuopio, Finland. His research interests are electrophysiology of the CNS and visual system.

Yang Dan received the Ph.D. degree from Columbia University, New York, NY, in 1994.

She is currently with the University of California at Berkeley, where her research group is interested in studying visual coding using a combination of experimental and computational techniques and in understanding mechanisms and functional consequences of activity-dependent plasticity in the adult brain.

Luke P. Lee received both the B.A. degree in biophysics and the Ph.D. degree in applied physics (major)/bioengineering (minor) from University of California at Berkeley (UC Berkeley).

He is an Assistant Professor in the Department of Bioengineering and Co-Director of Berkeley Sensor and Actuator Center at UC Berkeley. He has more than 10 years of industrial experience in microphotonic devices, holography, Superconducting Quantum Interference Devices (SQUIDs), and magnetic bioassays. His current research interests are nanogap biomolecular junctions, neural interfaces, integrated biophotonic devices, BioPOEMS (Bio-Polymer-Opto-Electro-Mechanical Systems) for lab-on-a-chip, Nano-POEMS for single molecule detection and manipulation. He has authored and coauthored over 60 journal and conference articles on integrated surface emitting laser diodes, SQUIDs, biomagnetic sensors, and nanogap DNA junctions for label free DNA detection.